NONLINEAR FINITE ELEMENT ANALYSIS OF STEEL MEMBERS UNDER VERY LOW- CYCLE LOADING

○ Yeon-Soo Park, Research Fellow, Disas. Prev. Res. Inst., Kyoto University
Satoshi Iwai, Research Associate, Disas. Prev. Res. Inst., Kyoto University
Hiroyuki Kameda, Professor, Disas. Prev. Res. Inst., Kyoto University
Taijiro Nonaka, Professor, Disas. Prev. Res. Inst., Kyoto University

1. INTRODUCTION In order to clarify damage and/or failure mechanism of steel members and their elements under severe seismic excitations, a series of experimental investigations on very low-cycle loading have been conducted by the authors[1]. Very low-cycle loading is meant to involve load repetitions of the order of a few to twenty cycles. The main purpose of this numerical analysis is to simulate quantitatively the hysteretic behavior of angle specimens such a loading, especially the history and cumulative state of local strains at their critical parts. The computer model is based on a three-dimensional, nonlinear hysteretic analysis by using MSC/NASTRAN program which includes the effects of the material and geometric nonlinearities. All computer runs have been made on the FUJITSU M-1800/30 computer system of Data Processing Center, Kyoto University.

2. MATHEMATICAL MODELING A typical finite element mesh is shown in Fig. 1 for an angle. The 4-noded quadrilateral isoparametric shell elements (QUAD4 elements) were used in modeling the tested part of the angle specimen. Both end-supporting parts of the specimen by holding the blocks[1] were modeled using the 3-noded stiff shell elements and the stiff QUAD4 elements for providing rigid-body motion in the vicinity of ends. The material property in this analysis has been assumed to be bilinearly etasto-plastic with kinematic hardening. The yield stress σ_y, Young's modulus E_s and Poisson's ratio ν were taken to be 349 N/mm^2, 2.06x10^5 N/mm^2 and 0.3, respectively. In the strain hardening region, the slope E_t of the stress-strain curve was selected 1% of E_s. The yield criterion of von Mises was used. The both ends of the test specimen were modeled as simply supported. As for the degrees of freedom, only the in-plane rotation was constrained in all the nodes of the model. The model comprised 306 shell elements. The models were subjected to cyclic enforced displacement Δ, in the contraction side (L3CP and L5CP model) and elongation side (T3CP model) with a constant amplitude 8% of the length l. The load was applied with small eccentricities, about ±0.5 mm distant from the gravity center at each end, in the Z-axis (Fig. 1), in order to produce a desired deflection mode as observed in the experiment, as shown in Fig. 2. The analysis was basically performed up to the number of cycles where cracks and/or the penetration of cracks through the thickness of the angle leg were observed in the experiment. The analysis for each model took about 3 hours of CPU time on the FUJITSU M-1800/30 machine on the average.

3. AXIAL LOAD-DISPLACEMENT RELATIONS
A comparison is made in Figs. 3 and 4 for the load-axial displacement relationship from the analysis and the experiment for the positive deflection mode. Here the load P and relative displacement Δ are normalized by the yield load N_y and length l, respectively. The analytical overall shapes show good agreement with the experimental results. In the case that loading was started from the contraction side (see (a) and (b) in Fig. 3), the compressive load-carrying capacity decreased suddenly after that the global buckling occurred at an early stage of the first cycle due to the inelastic local buckling. The compressive load-carrying capacities after the first cycle were significantly lower than the first buckling strength, but only a small decrease was seen in the succeeding tensile load-carrying capacities. In the case of cyclic loading started from a tensile displacement (Fig. 3(c)), the compressive strength in the first cycle was reduced considerably by plastic elongation and residual crookedness due to the eccentric tensile loading.

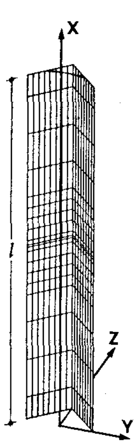

Fig. 1 Model.

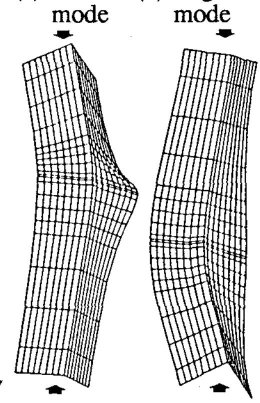

Fig. 2 Deformed shapes at Δ/l = -0.08.

4. TRACING OF LOCAL STRAIN HISTORY Figs. 5 and 6 show the axial stress-strain hysteresis and the plastic local strain history, respectively, on the inner and outer surfaces of the edge elements of the mid-height cross-section. The analytical results show that the maximum absolute local strain in the first cycle was in the range of 24-26% in the L3CP and L5CP model where loading was started in the

contraction side, and about 40% in T3CP, which started from the elongation side. The maximum absolute strain in the loading cycle, in which the first crack took place, was of the order of 27-30% in the cases of L3CP and L5CP, and 50% in T3CP. A trial computation was made for the summation of maximum plastic component of strain in the tensile stress side in each cycle, up to the outbreaks of crack indicated by the bold lines in Fig. 6. This attained the value of 110-230%. This numerical result corresponds to the residual local strain of 90-120%[1] at the ruptured portion under the monotonic-tensile testing. This sum, therefore, might be an indicator to represent the accumulated damage due to very low-cycle loading.

5. CONCLUDING REMARKS Using a finite element program, the results of a numerical analysis was presented for angle members under very low-cycles of loading. The overall behavior from the analysis shows good agreement with the experimental behavior. The local strain history was traced for large cyclic deformation by the numerical analysis. It is possible that this local strain information might be used to evaluate the seismic damage for steel members and their elements.

6. REFERENCE 1) S. Iwai, Y.-S. Park, T. Nonaka and H. Kameda : Very Low-Cycle Fatigue Tests of Steel Angle Members under Earthquake Loading, Proc. *10th World Conference on Earthquake Engineering*, Madrid, Vol. 5, pp. 2879-2884, 1992.

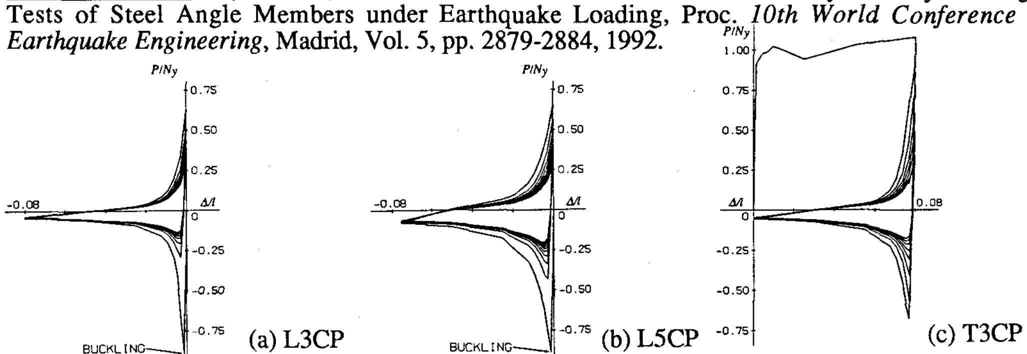

Fig. 3 Load-axial displacement relations [Analysis].

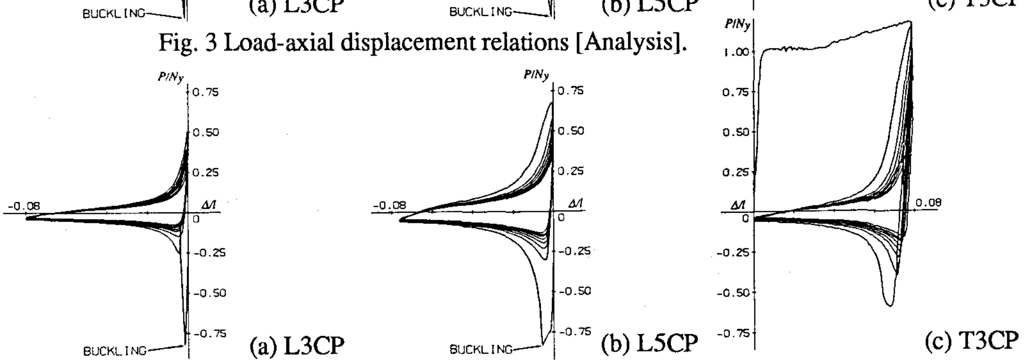

Fig. 4 Load-axial displacement relations [Experiment].

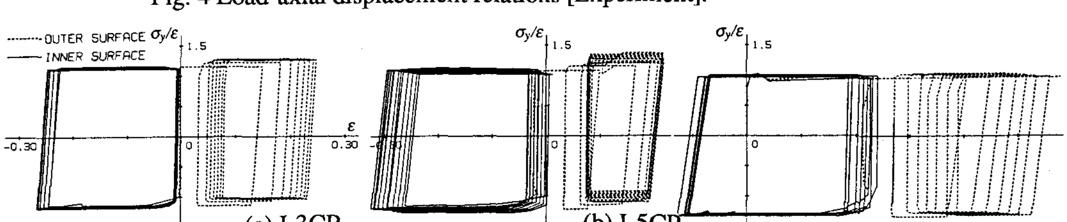

Fig. 5 Local stress-strain hysteresis [Analysis].

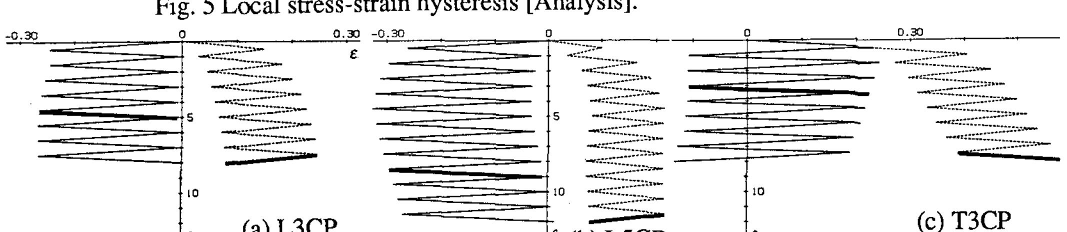

Fig. 6 Local strain histories with the increasing number of cycles [Analysis].